Granular packings sheared in an annular channel: Flow localization and grain size dependence

J.-C. Tsai[2,*] and J. P. Gollub[1,2,†]
[1]*Department of Physics and Astronomy, Haverford College, Haverford, Pennsylvania 19041, USA*
[2]*Department of Physics and Astronomy, University of Pennsylvania, Philadelphia, Pennsylvania 19104, USA*
(Received 14 February 2005; revised manuscript received 15 August 2005; published 14 November 2005)

We investigate experimentally a quasistatic flow of glass beads in an annular channel, in which particles are packed and sheared from above under a constant normal load. The experiments utilize techniques of refractive-index-matched fluorescent imaging to determine the motion of individual particles and the velocity fields inside the sheared packing. We demonstrated in a previous paper [Phys. Rev. E **70**, 031303 (2004)] that an ordering transition has a significant impact on the velocity profile. Here, we report the effects of layer thickness, channel width, and particle size on the internal velocity field. For very thin layers, the grain velocity exhibits a linear vertical profile. As the layer thickness increases, a strongly nonlinear velocity profile emerges, with particle motion that is largely localized to a narrow region (shear band) near the driving surface. Once the packing has reached its steady state, the velocity field is insensitive to the size of grains being used—the velocity profile does not scale with grain size. However, the vertical decay of grain velocity becomes significantly steeper as the horizontal width of the channel decreases. In addition, we demonstrate that changing the direction of shearing generates an anomalous mobility of grains in the deep interior that is sensitive to particle size. The transient grain motion is accompanied by an abrupt volume compaction and a gradual recovery as the shearing proceeds. Reviewing results from this and other works reveals that the velocity profiles of granular shear flows are often geometry specific. We present a heuristic continuum model that qualitatively captures the shear banding observed in this geometry.

DOI: 10.1103/PhysRevE.72.051304 PACS number(s): 45.70.−n, 83.50.Ax, 83.80.Fg

I. INTRODUCTION

Continuously flowing granular particles, such as flowing sands, seem to behave like fluids in a macroscopic sense. However, in comparison to ordinary fluids that are well described by the Navier-Stokes equations, the current understanding of granular flows is rather incomplete. This is especially true for slowly creeping or *quasistatic* flows, where particles are nearly in static equilibrium and are sustained by simultaneous contacts with multiple neighbors. Experimentally, there are few observations of grain motion inside three-dimensional (3D) dense packings. On the theoretical side, it has been a long-standing challenge to establish constitutive relations for the flow of packed grains whose interactions cannot be reduced to binary collisions as is conventionally done for granular gases.

One commonly observed but poorly understood property of creeping grains is the phenomenon of shear banding [1], i.e., the fact that the velocity of grains tends to be largely localized within a narrow region where the velocity field exhibits a strong spatial variation by many orders of magnitude within just a short distance. A particularly interesting question is what determines the length scale of the observed flow localization. One may be tempted to normalize the spatial coordinates of the velocity fields by the grain size. But so far neither a common functional form nor a universal spatial scale is found to be consistent with different experiments and computer simulations [2–18], for which we sample a few in Sec. IV and in the Appendix.

In this paper, we use the flow of packed granular particles in an annular channel as an example, to illustrate that grain size is not necessarily the dominant length scale for the velocity fields. Rather, the steady-state velocity field can depend substantially on geometrical factors such as the thickness and the width of the packing. Once the packing has reached the steady state, the velocity field is insensitive to the size of grains being used. In addition, we investigate the behavior of the packing in response to the change of shearing direction, which extends previous findings from two-dimensional granular flows [19] or grain motion observed at the free surface of a Couette cell [20] to the interior of a 3D granular packing. We find that the grain size does affect the response to the change of shearing direction.

It is possible that a sheared packing in its steady state can be modeled as a fluidlike continuum with its flow fields determined by the assumed local rheology and the confining geometry. We illustrate this possibility by presenting a heuristic model that qualitatively captures the shear banding observed in the annular channel, with the precaution that particle size may still be an important parameter in modeling transient flows. This paper extends our previously published works [21,22] that focused on the problem of shear-induced ordering of granular packings.

II. APPARATUS—A BRIEF DESCRIPTION

In this section, we briefly summarize the main features of our experimental system, which have been described in de-

*Present address: Department of Engineering Science and Applied Mathematics, Northwestern University, Evanston, IL 60208. Electronic address: jctsai@northwestern.edu
†Electronic address: jgollub@haverford.edu

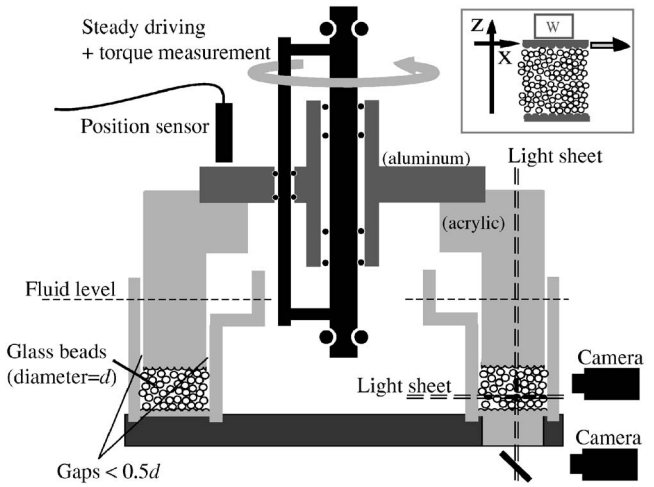

FIG. 1. Cross section of the annular shear cell, with the inset showing a schematic side view and the coordinates.

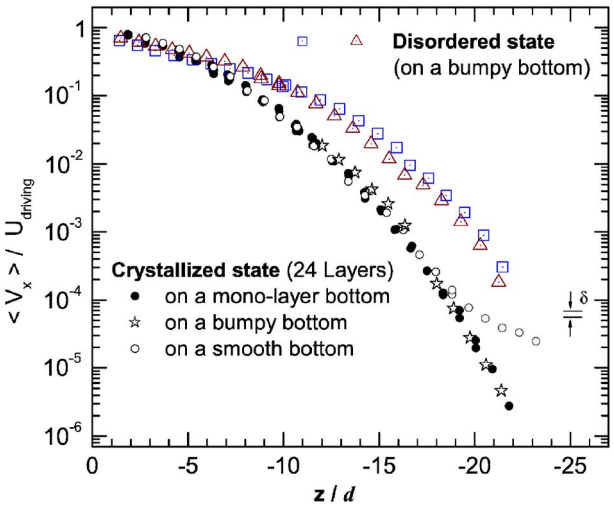

FIG. 2. (Color online) Vertical profiles of steady-state velocity for different states of order and with different boundary conditions. Velocities are normalized by the speed of the upper boundary near $z=0$. The symbol d represents the particle diameter 0.68 mm. For the 24-layer crystallized states, the data marks also indicate the average height of particle centers for each layer. The statistical variation over different sampling periods (corresponding to about $10^2 d$ of displacement accumulated locally) is about 30%, labeled as δ at the lower right. *For the crystallized state, the spatial decay of particle velocity is significantly steeper than that of the disordered state*. (The triangles and squares represent disordered-state velocity profiles measured during the same experiment but at two different vertical planes that are, respectively, 1/4 and 1/3 of the channel width from the sidewall.)

tail in Refs. [21,23]. As shown in Fig. 1, the apparatus consists of an annular channel with a rotating top that shears the glass beads from above while particles are packed under a fixed normal load. The typical diameter of the glass beads is $d=(0.68\pm0.03)$ mm, with the exception of some experiments where glass beads of diameter 1.0 mm or 2.0 mm are also used for comparison. The width of the annular channel is $28.5d$ and the circumference is about $800d$. The filling height is variable from a few particle diameters to $50d$. Cylindrical spacers can be installed in the channel to effectively narrow the channel for the purpose of comparisons. The glass beads are driven by a rotating ring-shaped upper boundary to which a monolayer of 0.68 mm glass beads has been glued. The bottom boundary can be adjusted to be (i) a monolayer of 0.68 mm beads, (ii) smooth, or (iii) bumpy—by gluing a mixture of particles of different sizes. Internal images are generated by the use of laser sheet illumination in presence of a fluorescent interstitial fluid whose refractive index matches that of the glass beads. The small gaps ($<d/2$) between the upper boundary and the sidewalls allow the fluid to flow through freely but prevent particles from leaving the region below. Therefore the vertical displacement of the upper boundary reflects the change of the total volume of the granular packing. The upper boundary constantly imposes a vertical load with a minimum of 1.3 Kg g. Please see Ref. [21] for further details.

III. EXPERIMENTAL RESULTS

In our experiments, the glass beads are driven over a wide range of driving speeds ($0.12d$/s–$12d$/s). Over this entire range of driving speeds and under the typical normal load (1.3 Kg g), the granular packing is entirely in the creeping or *quasistatic* state, as is estimated in the Appendix of Ref. [21]. The fluid drag even at the maximal speed is estimated to be negligible compared to the typical contact force between grains. The negligibility of the fluid drag is also consistent with the experimental fact that the velocity profiles are insensitive to two decades of change in driving speeds [22].

The primary effect of using the interstitial fluid, as opposed to using just dry particles, is perhaps the lubrication on the grain-grain and grain-wall contacts. We speculate that, in constructing a theory or simulation for quasistatically driven grains, the lubrication effect can be incorporated simply as a change in frictional coefficient in grain-grain and grain-wall contacts.

A. Steady-state velocity profiles

First, we briefly review the effect of crystalline ordering presented in our previous papers [21,22]. We show in Fig. 2 the vertical profiles of time-averaged velocity for different final states, produced by the use of different bottom boundary conditions and shearing protocols discussed in Ref. [21]. Note the strong shear banding (localization of velocity field) in both ordered and disordered states, as indicated by the decay of velocity from the top to the bottom by many orders of magnitude. Our measurements show that the downward decay of the mean velocity in the crystallized state is significantly steeper than in the disordered state and that, once ordered, the packing exhibits a velocity profile that is largely insensitive to different conditions of the bottom boundary, except for the lowest layers of particles. (The lowest layers of particles appear to slide more on a smooth bottom than in other cases. Further examples are shown in Fig. 4.)

We extend our previous investigations and demonstrate in Fig. 3 the velocity profiles for packings of different geo-

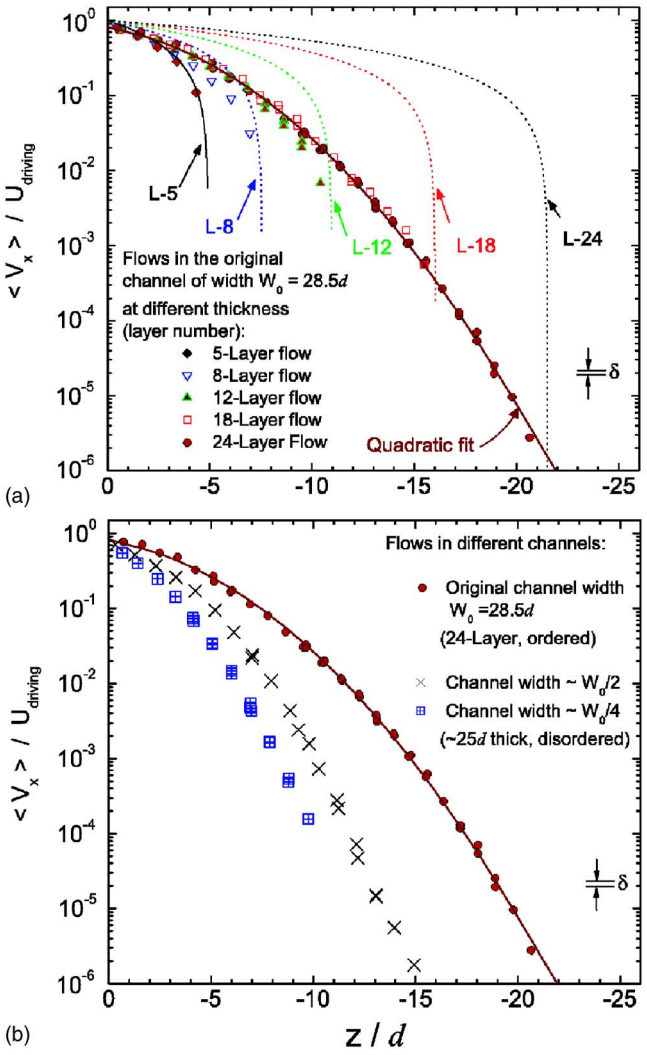

FIG. 3. (Color online) Vertical profiles of the steady-state velocity in sheared packings of different sizes. Velocities are normalized by the speed of the upper boundary at $z=0$. The particle diameter d is 0.68 mm. (a) Dependence on thickness: Different labels represent particle velocity profiles at different packing thickness, whereas the curves labeled as L-n represent the hypothetical linear relation $\langle V_x\rangle/U=|1-z/H|$ with H being the total height of an n-layer packing. For thick layers, the profile approaches a master curve $\langle V_x\rangle/U=0.798\exp[0.103(z/d)-0.023\,75(z/d)^2]$ which has a quadratic function of z in its exponent. Note that for thin layers, the velocity profile deviates substantially from the initial segment of the master curve, illustrating the effect of a finite depth. In the extreme case of just five layers, the particle velocity profile almost coincides with the linear relation (curve L-5). (b) Dependence on the channel width. Note that *decreasing the channel width produces steeper velocity profiles*.

metrical parameters—thickness and width. In Fig. 3(a), the thickness of the packing is varied by filling the channel with different amounts of glass beads. The packings form crystallized states of 5, 8, 12, 18, and 24 layers, respectively, after being sheared for a long time with the monolayer bottom boundary condition. For a packing as thin as five layers of material, the velocity profile is almost linear (see the reference curve L-5). As the thickness is increased, the velocity

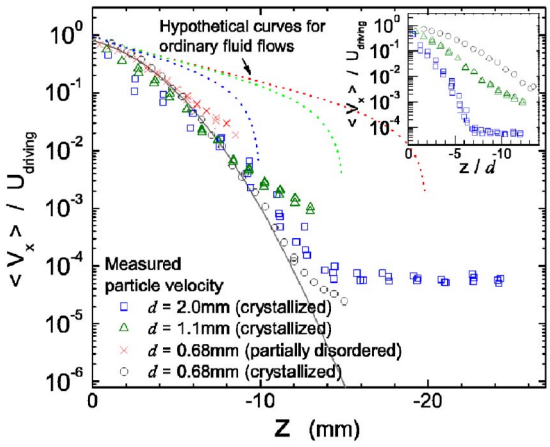

FIG. 4. (Color online) Vertical profiles of steady-state velocity for particles of different sizes. The time-averaged velocities $\langle V_x\rangle$ are normalized by the speed of the driving boundary and plotted against vertical position z. All experiments are performed with a smooth bottom boundary. Horizontal positions of data labels indicate the heights of individual layers, with the exception of the data represented by crosses (which is partially disordered). The quadratic master curve (see Fig. 3) is shown in light gray. The height $z=0$ represents the height of the driving boundary. Theoretical velocity fields of ordinary fluids in the same channel, with three different assumed positions of the lower boundary ($z=-10$ mm, -15 mm and -20 mm), are averaged over the channel width and plotted as functions of z for comparison. The upper portion of the velocity profiles show that *the spatial decay rates of particles of different sizes are similar*, and are generally steeper than that of an ordinary fluid driven in an annular channel of the same width. The inset shows that the measured particle velocity profile does not scale with particle size d.

profile progressively deviates from the linear relation, as can be seen in Fig. 3(a) by comparing the data points with the corresponding curves showing the hypothetical linear relations for thicker packings. The velocity profile for thick packings eventually approaches a limiting master curve, which can be well fitted by a quadratic function of z on this semilog plot (see caption).

In the experiments shown in Fig. 3(b), installation of a transparent cylindrical spacer within the annular channel divides it into two channels with widths that are narrower by factors of 2 and 4 than the original one. The ordered state ceases to exist in the narrowed channels. The grain velocity in these disordered states also depends in part on the horizontal position (see Fig. 4 of Ref. [22]); therefore the velocity profile also depends on the imaging plane. The vertical profiles shown in the graph are measured along vertical planes that pass through the center of each channel, where grains move the fastest. Figure 3(b) indicates that decreasing the channel width generally produces a steeper velocity gradient, despite the fact that disorder favors weaker gradients (Fig. 2). This observation suggests that sidewall resistance should play an important role in determining the velocity field, as we emphasize in Sec. IV B.

Figure 4 shows the measurements of the time-averaged velocity fields using different sizes of monodisperse spherical glass beads. The data points here include experiments

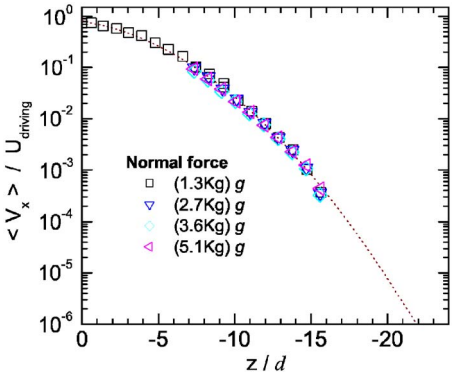

FIG. 5. (Color online) Vertical profiles of steady-state velocity for particles under different normal loads. The effective weight of the grains immersed in the fluid is 0.0875 Kg g. The time-averaged velocities $\langle V_x \rangle$ are insensitive to the change of normal force by a factor of 4. (Conditions: 0.6 mm particles; 18-layer ordered state in the $28.5d$-wide channel; driving speed$=12d/$s. The dotted line represents the master curve from results of thicker packings, as shown in Figs. 2–4.)

using three different particle sizes with a comparable number of layers (14 or 15), as well as the profile of a 24-layer flow as a reference. We find that the velocity decays of packings composed of different particle sizes follow roughly the same trend in terms of physical distance from the driving surface. *Even though particle diameter d may seem to be a convenient length to nondimensionalize coordinates, the inset shows no clear advantages of doing so* in these cases. In addition, we include in the graph the hypothetical profiles for ordinary fluids in the same channel for three sample thicknesses. These curves are obtained by solving the corresponding Laplace equation in a rectangular geometry and then averaging across the channel [23]. All curves have a primary decay length $\lambda_1^{-1}=(W_0/\pi)$ set by the channel width W_0. Note that either for the ordered flows shown here or for the disordered flows (Fig. 2), the velocity decay of granular flows is generally steeper than what is expected of an ordinary fluid driven in the same channel.

All experiments shown in Fig. 4 are performed with a smooth bottom boundary, so that the lower portion of the grain velocity profiles also exhibits an additional feature: near the smooth bottom, these profiles tend to somewhat flatten, presumably because the smooth bottom allows the grains to slide more easily. In the extreme case of 2 mm beads, the lowest six layers slide almost as a solid block—see Sec. IV B for further discussions.

We change the normal load by adding extra weight on top of the upper boundary up to roughly four times the typical load (1.3 Kg g), and find no detectable change in the velocity profiles, shown as Fig. 5. The weight of the grains, which in these cases is 0.0875 Kg g when immersed in the fluid, is expected to cause a small gradient of normal stress, with the fractional change of stress inversely proportional to the imposed normal force. The observed invariance of the velocity profile therefore implies that a fractional change of normal stress of the order of 10^{-1} due to grain weight is insignificant, compared to the effect of the channel width [Fig. 3(b)] and the internal state of ordering (Fig. 2).

B. Response to change of shearing direction

The behavior of grains in response to the change of shearing direction provides further insight into quasistatically driven granular flows. As shown in Fig. 6, we investigate the response to the change of shearing direction by first driving the boundary steadily in one direction (for more than 10^2d of total translation), stopping the motion, then restarting the boundary motion in the reverse direction. As soon as the driving boundary starts to move in the reverse direction, the grains in the interior exhibit a short period of anomalous mobility [Figs. 6(b) and 6(c)], compared to the motion in the steady state [Fig. 6(a)]. Figures 6(d)–6(f) show the average motion of particles over the course of time t, accompanied by the measured change of total volume: The amplitude and the duration (scaled by $|U_0|$) of the anomalous mobility are roughly independent of the driving speed for the two decades of $|U_0|$ being used, as shown in Figs. 6(d) and 6(e). (In the curves representing grain velocities, the small spikes are due to measurement noise. The grains are completely static when the driving boundary is at rest.) Figure 6(f) shows the vertical displacement of the upper boundary, which indicates the change of total volume in response to the shear reversal. The granular packing first exhibits a step compaction accompanying the anomalously mobile period, then shows a more gradual recovery as the shearing continues in the reversed direction. The full recovery to the prior volume requires a large total displacement of the driving boundary (about 10^3d–10^4d, see Refs. [21,23]); this phenomenon indicates that the state of the packing continues to evolve far beyond the brief period of anomalous mobility. Both the crystallized and the disordered packings exhibit similar behaviors in response to the reversal of boundary driving.

In addition, inspecting the images at high frame rates reveals that the initiation and stopping of the grain motion in the entire bulk as thick as 24 layers are effectively instantaneous; there is no detectable propagation delay beyond the time resolution corresponding to the boundary motion of about $0.1d$. The observation of the rate-independent, nearly instantaneous transient motion inside the granular packing, combined with the steep compaction and gradual recovery, is consistent with the picture of quasistatic jammed solids: upon reversal of the shearing, the packing first unjams then rejams with its anisotropy readjusted to reflect its new direction of shearing.

Interestingly, we find that the degree of this anomalous mobility in response to the change in shearing direction depends sensitively on the grain size: by progressively increasing the particle size, this anomalous mobility can be substantially suppressed. For example, using 14 layers of 2 mm particles, we find that this phenomenon becomes undetectable, while the cases of 0.68 mm particles with either a comparable layer number or physical thickness in the vertical direction exhibit the anomalous transient motions shown in Figs. 6(a)–6(c) and 6(e). The implication of this particle size effect is further discussed in Sec. IV A. In addition, the total thickness also affects the degree of this anomalous transient motion: in the case of 0.68 mm particles, about 13 layers or more is required for the effect to become detectable [23].

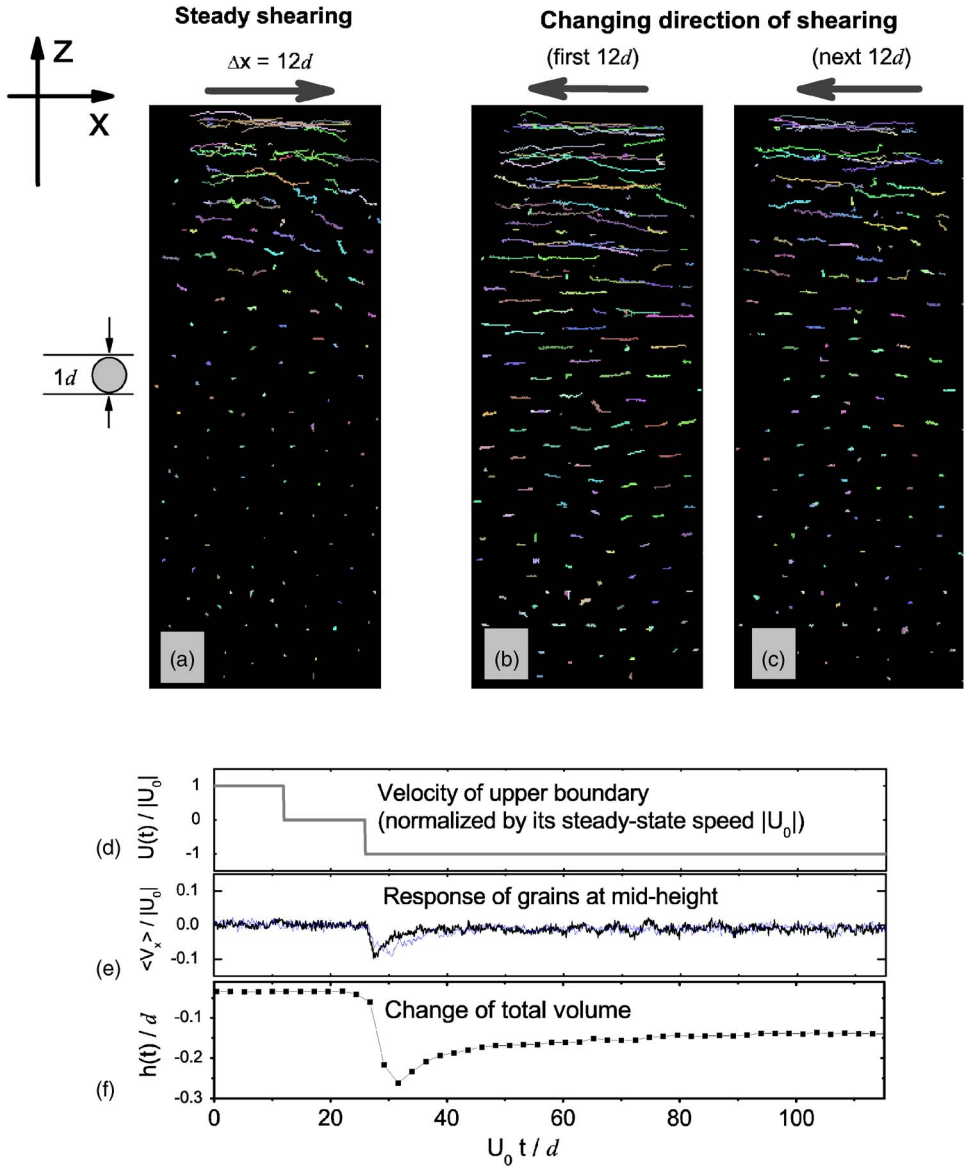

FIG. 6. (Color online) Time-resolved response of individual particles in an internal slice, upon the change of shearing direction, and the corresponding change of total volume. The thickness of the packing is equivalent to 24 layers of particles. (a)–(c) The trajectories of individual particles captured at a vertical internal slice within a period corresponding to $12d$ of boundary displacement, during the steady shearing (a), immediately following the reversal (b), and during the next period (c). The upper edges of the images coincide with the approximate position of the driving boundary. (d)–(f) The typical shearing protocol (d), the velocity of grains at mid-height (e), and the corresponding change of total volume (f). $|U_0|$ stands for the steady-state driving speed. Prior to the time $t=0$, the packing has been steadily sheared by the upper boundary in the positive direction with a total displacement more than $10^4 d$. Graph (e) shows the averaged velocity of 60 particles in a horizontal slice at mid-height, as a function of time. Data from experiments using two driving speeds differing by a factor of 100 ($12d$/s and $0.12d$/s) are overlaid to show that the amplitude of the anomalous mobility and its duration (scaled by the boundary displacement) are insensitive to the change of driving speed. Graph (f) shows the vertical displacement of the upper boundary $h(t)$, with $|U_0|$ being $12d$/s; the curve indicates an abrupt compaction of total volume followed by a gradual recovery.

IV. DISCUSSION

A. Effects of particle size in experiments

We have demonstrated that, while the vertical decay of velocity depends sensitively on the channel width [Fig. 3(b)] and the state of internal ordering (Fig. 2), the velocity gradient is insensitive to change of particles size by a factor of 3 (Fig. 4). These observations suggest that the time-averaged flow field of the packing in its steady state may be understood as the behavior of a continuous effective medium, with its cross-sectional profile determined mainly by specifying the conditions imposed at the boundary—in analogy to the case of fluid driven in a finite-sized channel. While this conjecture does not preclude particle size as a parameter in a general theory, we expect that the particle size does not affect the *steady-state* velocity field significantly. In Sec. IV B, we present a heuristic theory for the steady-state velocity profile that does not depend on particle size.

In contrast to the steady-state velocity field developed after a prolonged shearing, the particle size does affect the transient response following a change of shearing direction. We pointed out in the previous section that increasing the particle size can suppress or eliminate the anomalous mobility shown as Figs. 6(a)–6(c) and 6(e). In this sense, treating the granular packing as merely a continuous fluid-like medium regardless of its grain size is insufficient. It may not be surprising that at a small distance scale, especially when the boundary driving involves reversals that induce the relaxation and reestablishment of the grain contact networks, the particle size is relevant, whereas at a large distance scale the "granularity" of the medium can be smoothed out by averaging: At a large distance scale, which is by definition how the steady-state velocity field is determined, the packing flows more like a fluid, with its velocity field primarily controlled by the geometrical factors of the system. This behavior may be analogous to the common observation that, in the most general sense, whether a deforming medium should be described as an elastic solid or viscous fluid depends on the scale of deformation (or the time scale).

B. A heuristic model for the steady-state velocity profile

The shear banding of granular flows, i.e., the localization of shear within a narrow band in which the local shear rate (and the velocity itself) varies by orders of magnitude, is a commonly observed phenomenon. But questions such as what determines the location of the shear band and what parameters control the length scale of the velocity variation, i.e., the *width* of the shear band, do not seem to have a simple answer that fits all contexts. The experimental results by Mueggenburg [11] suggest that the occurrence (and location) of a shear band in granular materials driven between two parallel boundaries can be highly sensitive to a slight asymmetry in its experimental setup. Recent experiments by Fenistein *et al.* using a split-bottom Couette cell [15] have also demonstrated that a shear band does not necessarily occur near the boundary of the packing: depending on the geometry of the shear cell, a narrow shear band in the form of a curved surface in the interior of a granular packing can be generated and sustained indefinitely. In the Appendix, we sample more experiments and theories of granular flows in different geometries, plus relevant computer simulations not limited to granular flows, to illustrate the wide spectrum of mechanisms that result in shear banding [2–18]. These investigations show that the velocity profile of sheared granular packings is often geometry specific. It is therefore not surprising that, among all existing results including ours, there has been neither a common functional form of the velocity profile, nor a universal characteristic length scale in units of the grain size d, which sometimes appears to be just a convenient choice of parameter to normalize the spatial coordinate but implies no particular universality.

In what follows, we describe a heuristic model that seems to capture the shear banding of the steady-state velocity field in our geometry. Motivated by the observations that the velocity decays more strongly with depth in the narrower channels (Fig. 3), and that the velocity decay is insensitive to the change of particle size (Fig. 4), we base the model on the balance established between the shear resistance at the sidewalls (particle-wall friction) and the internal shear stress (friction between particles), accompanied by simple rheological assumptions. The slowly deforming granular packing is modeled as a continuous effective medium with no explicit reference to the particle size.

For illustrative purpose and mathematical simplicity, we restrict our discussion to the ordered state, because in this case particles are interlocked horizontally as semirigid sheets so that the velocity field V_x depends only on the height z but not on the position across the channel. The notation σ_{xz} stands for the shear stress at each height. Both the velocity and stress discussed here are coarse grained and time averaged. The z axis points vertically upwards, with $z=0$ representing the driving boundary at the top, and the shear rate $\dot{\gamma}=V_x'(z)$. The shear resistance exerted by the sidewall per unit area is represented by $\sigma^{\text{wall}}(z)$. Also for illustrative purposes, the present discussion is restricted to a channel with an infinite depth so that the simple condition $V_x(-\infty)=0$ can be assumed, even though generalization to the finite-depth case is feasible when appropriate boundary conditions governing the grain-wall interactions at $z=0$ and $z=-H_0$ are given.

By considering the stress balance for a stationary state, we have

$$[\sigma_{xz}(z)-\sigma_0]W_0 = 2\int_0^z \sigma^{\text{wall}}(z')dz' \tag{1}$$

in which $\sigma_0 \equiv \sigma_{xz}(0)$, and W_0 represents the channel width. We have assumed that the friction on the smooth sidewall $\sigma^{\text{wall}}(z)$ is sufficiently small that, for an extended range of height $0>z>-|Z_*|$, the change in the shear stress $\sigma_{xz}(z)$ with respect to z is not too large. More specifically, we assume that

$$\left| 2\int_0^{-|Z_*|} \sigma^{\text{wall}}(z')dz' \right| \ll |\sigma_0 W_0| \tag{2}$$

for an extended region $[-|Z_*|,0]$, so that $\sigma_{xz}(z)$ within this region is expected to be always greater than the yield stress [24]. We are only interested in the velocity field $V_x(z)$ within this region.

As a first approximation, one may assume that the grain-wall friction can be approximated by a height-independent constant, $\sigma^{\text{wall}}(z)\approx\sigma_1$, so that the right hand side of Eq. (1) is just a linear function of z. Then a sharp shear band emerges if one further assumes that the internal shear stress $\sigma_{xz}(z)=f(\dot{\gamma})$ depends only very weakly on the local shear rate $\dot{\gamma}$, in the sense that a small decrease of σ_{xz} requires a decrease in $\dot{\gamma}$ by orders of magnitude. This assumption can be expected to be true for most frictionlike materials, especially packed grains. In principle, an arbitrarily sharp shear band would occur as a result of assigning an arbitrarily weak rate dependence to the shear stress of the material inside the channel.

Although the occurrence of a sharp shear band does not demand a specific functional form of $f(\dot{\gamma})$, in what follows we use a logarithmic function to represent the weak rate dependence [25], i.e., $\sigma_{xz}=f(\dot{\gamma})\approx\sigma_0[1+\alpha\ln(\dot{\gamma}/\dot{\gamma}_0)]$ where α is a small positive constant, to illustrate one possible way of producing the strongly localized velocity profile. Solving Eq. (1) with the constant-sidewall-resistance approximation and the logarithmic representation of $f(\dot{\gamma})$ gives an exponential shear-banding profile

$$V_x(z)\approx V_x(0)\exp\left(\frac{z}{\frac{\alpha}{2}(\sigma_0/\sigma_1)W_0}\right) \tag{3}$$

when the boundary condition $V_x(-\infty)=0$ is imposed.

A quantitative comparison of theoretical predictions to the experimentally measured nonexponential profiles (Figs. 2–4) would require further improvements of the model (as discussed in the next paragraph) and some estimates of the material parameters [26]. Nevertheless, this simple exponential solution illustrates some important features: (i) The channel width W_0 affects the spatial scale of the velocity decay; this is qualitatively consistent with the our measured velocity profiles with narrowed channels [Fig. 3(b)]. (ii) Increasing the factor σ_0/σ_1 would decrease the velocity gradient. The use of the interstitial fluid is likely to increase this factor because σ_1 represents the tangential force as beads slide against the glass walls and should be more sensitive to fluid lubrication than σ_0, of which we expect a substantial portion is contributed by force components that are normal to the local contact surface between grains of the packing and the particles glued on the driving surface. In our experiments, the dramatically longer timescale for the crystallization of dry than that of fluid-immersed particles, reported in Ref. [22], is consistent with this interpretation.

To reproduce the observed nonexponential profiles shown as the downward bending curves on the semilog plots (see Fig. 3 for a curve fitting), improvements of the model are needed. There is no unique approach, and an accurate answer may require a combination of them, for example: (i) modifying the functional form of $f(\dot{\gamma})$—see endnote [25]; (ii) introducing a slip-speed dependence for the sidewall resistance $\sigma^{\mathrm{wall}}(z)$—see endnote [27]; and (iii) including the effect of the vertical variation of normal stress (due to weight of grains) on $\sigma_{xz}(z)$ and $\sigma^{\mathrm{wall}}(z)$, and subsequently its effect on the sidewall friction.

Note that the nonlinear vertical decay of velocity field by orders of magnitude is a characteristic of the channel geometry in which the sidewalls provide substantial resistance, *regardless* of whether granular particles or ordinary Newtonian fluids are being used. (The flow field for ordinary fluids in this geometry can be determined by finding the stationary solution of the Navier-Stokes equation with no-slip boundary conditions [23]. For both granular flows and ordinary fluid flows, the primary decay length is expected to be proportional to the channel width W_0.) However, the granular decay length is much shorter than the fluid decay length (see Fig. 4), a result that is captured by the heuristic model as a consequence of the weak rate dependence $f(\dot{\gamma})$. The weaker the rate dependence of the shear stress, the sharper the resulting shear band. (See, for example, the effect of a small α on the delay length derived from our heuristic model.)

In this model, the sidewall interaction breaks the symmetry between the upper and lower boundaries (discussed in the Appendix with greater detail) and causes the shear band to occur in the vicinity of the top boundary. Nevertheless, gravity (the weight of grains) causes some gradient in normal stress and thereby may also contribute to the asymmetry and shear banding. However, the observed invariance of velocity profile with respect to substantial changes in normal force (Fig. 5) suggests that the change of internal normal stress along the height of the packing, estimated to be at most 10% of the imposed stress, is secondary to the effect of the sidewall resistance. The asymmetry induced by the normal stress gradient is therefore ignored in the simplest version of our model.

Further discussion of the model can be found in the thesis work listed as Ref. [23]. Here, we conclude with two additional remarks: (i) The horizontal coherence, which is characteristic of the ordered state that occurs for a range of packing thickness and channel width with suitable bottom conditions, allows a one-dimensional ordinary differential equation (ODE) model depending only on the height z. For a disordered state in which the velocity field exhibits gradients in both the vertical and horizontal directions, a full 3D treatment with partial differential equations (PDEs) would be required. This complication should be taken into account in predicting flow fields in the limits of very wide or very thick channels, where the horizontal coherence is expected to break down and only disordered states can exist. (ii) Our model applies to an upper portion of the packing limited by $[-|Z_*|,0]$ defined in Eq. (2). For very thick packings, the internal shear stress may go below yield stress at locations lower than some critical depth so that the lower portion of the packing becomes a rigid block. This may explain the solid block observed at the lower portion of the packing composed of 2 mm particles shown in Fig. 4. Interestingly, a solid block motion has also been observed in the 2D simulations by Thompson and Grest [28]—however, an important difference is that our experiments are performed at low speeds and with a heavy normal load so that the entire packing is uniformly in a quasistatic state, whereas in their simulations some upper portion of the layer can be in a collisional state contrasting the slowly creeping (or even static) lower portion.

V. CONCLUSION

In this work, we use a packing of glass beads in an annular channel to investigate quasistatic flows of granular materials. The internal velocity fields are determined over a wide dynamical range; the transient behavior in response to the reversal of driving motion is also studied. The velocity profiles exhibit effects of the system geometry: In the limiting case of a very thin packing, the grain velocity exhibits merely a linear dependence on location between the driving boundary to the static bottom. For sufficiently thick packings, the grain velocity exhibits a strongly nonlinear profile

or shear band that reflects not only the internal state of ordering but also the effect of channel width. However, the steady-state velocity profile is *insensitive* to the change of particle size. These observations, accompanied by analyses of other previous studies, show that the grain size is not necessarily the dominant length scale for determining the velocity fields of a granular flow and that the system geometry can dominate instead. This may explain why a universal decay length cannot be found by simply normalizing the spatial coordinates in all granular flows with the grain size.

We show that an anomalous mobility of individual grains in response to changes of shearing direction can be detected inside the deep interior of a three-dimensional granular packing, reflecting the rearrangement of internal grains to adapt to the new shearing direction. Furthermore, our simultaneous volume measurements demonstrates that the anomalous mobility is accompanied by an abrupt compaction and subsequently a gradual recovery, which may be regarded as a sensitive indicator of the slow evolution induced by prolonged shearing.

Our experiments, as well as the continuum heuristic model, suggest that the nonlinear spatial decay of the velocity field is a characteristic of channel flows, regardless of the materials (grains or fluids) being driven. Nevertheless, the phenomenon that the observed grain velocity profile exhibits a *much steeper spatial decay* than what is expected for an ordinary fluid driven in the same channel can be attributed to a particular non-Newtonian property which is perhaps unique to granular materials—the insensitivity of shear stress to the local strain rate. In a steady state, the slowly deforming granular packing in the channel can be modeled as an effective continuum that is insensitive to the particle size. On the other hand, we find from our experiments that the transient mobility in response to changes of shearing direction exhibits a considerable dependence on the grain size.

ACKNOWLEDGMENTS

This work is supported by NSF Grant Nos. NSF-DMR-0405187 to Haverford College and NSF-DMR-0079909 to the University of Pennsylvania. The authors appreciate the helpful interactions with Tom Lubensky, Arjun Yodh, and John Crocker. J.C.T. is indebted to Michel Louge, H. M. Jaeger, Bob Behringer, and Karen Daniels for fruitful discussions, and to Sascha Hilgenfeldt for providing a stress-free environment to complete this manuscript.

APPENDIX: SHEAR BANDING IN THEORIES AND EXPERIMENTS

In this section, we review shear banding from both theoretical and experimental points of view. The purpose of this section is to illustrate the diverse factors that generate a shear band, thereby causing velocity profiles to vary from system to system.

On theoretical grounds, the simplest model system for sheared grains appears to be a two-dimensional (2D) collection of grains steadily sheared between two parallel identical walls, with no other interactions except grain-grain and grain-wall contacts. Since the model system is symmetrical along the midplane between the two shearing walls, the simplest time-independent treatment would predict a velocity profile that is antisymmetrical in an inertial frame that comoves with the grains along the midplane. Aside from a simple linear profile that would obviously satisfy such symmetry, examples of nonlinear solutions exist in the literature, e.g., Ref. [2]. Any time-independent, nonhysteretic treatment of this type would preclude the localized one-sided shear banding that is commonly seen in experiments.

There are molecular dynamics (MD) simulations that generate a one-sided shear banding, where the midplane symmetry is broken in one way or another. The initial condition often generates the required symmetry breaking and the shear banding in computations that simulate how a collection of grains evolve. In the constant-normal-stress simulations listed as Ref. [3], grains are initially all static with respect to one boundary: depending on the stress level, the system can develop either a smooth nonlinear velocity profile or abrupt shear bands in the interior. There are also similar examples in the constant-volume simulations listed as Refs. [4–6], while related work reported in Ref. [7] provides an example in which one boundary is gradually pushed inwards. Notably, the shear banding in constant-volume simulations often exhibits some rate dependence: For instance, in Ref. [4], a simulation of athermal particles, shear banding occurs only when the shear rate exceeds a threshold set by the sound speed of the colliding particles, whereas the shear banding of thermal particles in Refs. [5,6] occurs only at low driving speeds. Another frequently encountered symmetry breaking factor is a body force such as gravity that points towards one of the boundaries. The shear banding in theories and simulations under a constant stress reported in Ref. [9] requires gravity, and the velocity would show a linear profile when gravity is turned off [10]. In addition, in comparing different simulations and experiments, it is important to keep in mind that the situation of a collection of grains under a heavy constant stress and a slow shear rate (like our quasistatic flows) can be fundamentally different from that of constant-volume simulations in the low-speed limit [8].

Physical experiments on granular flows often involve static confining walls that exert some drag on the flowing grains. The drag can be an important or even dominant factor that breaks the symmetry and controls the shear banding profile. One recent experiment utilizes a symmetrical setup with a stack of independently movable slats, such that grains are sheared between two parallel plates moving at different speeds, while the confining walls freely conform to the granular packing [11]. The grain velocity profile as the shearing starts is found to be nonunique and sensitive to the state of packing; the observed velocity field ranges from a linear relation with position to a sharp shear band only a few particle diameters wide. However, it is also found that a shear band consistently develops at the faster moving wall in this apparatus as the shear strain accumulates, illustrating that a small residual asymmetry such as the small mechanical vibration in this experiment can have a profound effect that controls the shear banding.

Granular flows in a conventional Taylor-Couette cell [12–14] have an intrinsic asymmetry along the principal gra-

dient of velocity. This curvature effect can be a controlling factor for shear banding. Based on the macroscopic balance of angular momentum, the steady-state local shear stress ($\sigma_{\theta r}$) is inversely proportional to the square of the distance (r) from the apparatus axis. It is therefore not surprising that a large velocity gradient tends to accumulate around the inner cylinder, where the shear stress is relatively large so that materials "yield" more easily. Ref. [2] gives an example showing that including the effect of curvature in a theory can reproduce the one-sided shear banding observed in experiments. In a real experiment, other relevant factors such as the static bottom, the upper free surface, and the weight of grains can further complicate the problem. Experiments using a modified Couette cell with a split-bottom design illustrate the profound effect of the bottom [15]. The locus of the shear band in Ref. [15] has been reproduced successfully by theorists [16] using a variational principle based on the minimization of frictional dissipation. (But note that in this particular theory the shear band is defined as a zero-width surface, leaving the velocity decay profile within the shear band irrelevant.)

Gravity-driven granular flows on an inclined channel formed by parallel vertical sidewalls usually consist of a thin rapidly flowing surface layer and a creeping bulk region below. The velocities of grains near the sidewalls have been measured using very wide channels [17] or narrow channels [18]. Both the sidewall resistance and the gradient of normal stress caused by the self-weight of the pile can be important in controlling the measured velocity profile. Interestingly, Ref. [18] reports that the thickness of the rapidly flowing surface layer scales approximately with the distance between the sidewalls. This observation is somewhat related to our experiments using different channel widths (Fig. 3), except that our measurements focused on resolving the profile of the slow creep, while in the model discussed in Ref. [18] the region below the rapid flowing layers is treated as a solid.

This review of previous work suggests that the profile of velocity decay in experimental granular shear flows depends strongly on the system geometry. It may explain why simply rescaling the spatial coordinates by particle size does not lead to a universal profile in different experiments.

[1] In the work described in this paper, we focus on the shear banding of continuous flows. In the literature, the term shear band has also been used in different contexts, such as the strain localization observed in the biaxial or triaxial tests of granular solids when a finite strain is applied and failure planes are generated—see K. A. Alshibli, S. N. Batiste, and S. Sture, J. Geotech. Geoenviron. Eng. **129**, 483 (2003), for example.

[2] L. S. Mohan, K. K. Rao, and P. R. Nott, J. Fluid Mech. **457**, 377 (2002).

[3] E. Aharonov and D. Sparks, Phys. Rev. E **65**, 051302 (2002).

[4] N. Xu, C. S. O'hern, and L. Kondic, Phys. Rev. Lett. **94**, 016001 (2005).

[5] F. Varnik, L. Bocquet, J.-L. Barrat, and L. Berthier, Phys. Rev. Lett. **90**, 095702 (2003).

[6] J. Rottler and M. O. Robbins, Phys. Rev. E **68**, 011507 (2003).

[7] L. Kondic, *Proceedings in 21st International Congress of Theoretical and Applied Mechanics (ICTAM)*, Warsaw, Poland (August 2004), edited by W. Gutkowski and T. A. Kowalewski, IPPT PAN, Warszawa.

[8] C. S. Campbell points out that there is no path between inertial (rapid) flow and quasistatic flow by varying the shear rate at a fixed concentration. See C. S. Campbell, J. Fluid Mech. **465**, 261 (2002).

[9] D. Volfson, L. S. Tsimring, and I. S. Aranson, Phys. Rev. E **68**, 021301 (2003).

[10] L. S. Tsimring (private communication).

[11] N. Mueggenburg, Phys. Rev. E **71**, 031301 (2005).

[12] D. M. Mueth *et al.*, Nature (London) **406**, 385 (2000).

[13] D. M. Mueth, Phys. Rev. E **67**, 011304 (2003).

[14] L. Bocquet *et al.*, Phys. Rev. E **65**, 011307 (2001).

[15] D. Fenistein, J. W.van de Ment, and M. van Hecke, Phys. Rev. Lett. **94**, 094301 (2004).

[16] T. Unger, J. Torok, J. Kertesz, and D. E. Wolf, Phys. Rev. Lett. **92**, 214301 (2004).

[17] T. S. Komatsu, S. Inagaki, N. Nakagawa, and S. Nasuno, Phys. Rev. Lett. **86**, 1757 (2001).

[18] N. Taberlet *et al.*, Phys. Rev. Lett. **91**, 264301 (2003).

[19] B. Utter and R. P. Behringer, Eur. Phys. J. E **14**, 373 (2004).

[20] W. Losert and G. Kwon, Adv. Complex Syst. **4**, 369 (2001).

[21] J.-C. Tsai and J. P. Gollub, Phys. Rev. E **70**, 031303 (2004).

[22] J.-C. Tsai, G. A. Voth, and J. P. Gollub, Phys. Rev. Lett. **91**, 064301 (2003). We refer to the ordering as "crystallization," even though the ordering is primarily in hexagonal layers that slide over each other, so the ordering is less complete than would be the case for a true three-dimensional crystal.

[23] J.-C. Tsai, Ph.D. thesis, University of Pennsylvania, Philadelphia, 2004. See EPAPS Document No. E-PLEEE8-72-076511 for a description of the main features of our experimental system. This document can be reached via a direct link in the online article's HTML reference section or via the EPAPS homepage (http://www.aip.org/pubservs/epaps.html).

[24] In most cases, we expect that $[-|Z_*|,0]$ extends to the entire packing of thickness H_0: With the constant-friction approximation $\sigma^{\mathrm{wall}}(z)\approx\sigma_1$, this condition is equivalent to $2\sigma_1 H_0/\sigma_0 W_0 \ll 1$, which is expected to be true when $\sigma_1 \ll \sigma_0$ (due to the combination of the smoothness of the sidewalls and the lubrication of interstitial fluid) and $H_0 \sim W_0$ (e.g., in the typical case where 24 layers of particles are sheared in the $28.5d$-wide channel).

[25] R. R. Hartley and R. P. Behringer, Nature (London) **421**, 928 (2003). As is pointed out by the authors, although the logarithmic expression can be a good approximation within a range of shear rates, modification is needed to address the issue that shear stress is expected to approach a constant (rather than infinity) as the shear rate approaches zero.

[26] The simple exponential form gives a length $(\alpha\sigma_0/2\sigma_1)W_0$, while the local slopes of the measured nonexponential velocity profile on the semilog plots (Fig. 3) indicate a range of length

scale from $0.03W_0$ to $0.3W_0$. The ratio (σ_0/σ_1) is expected to be greater than unity, because the shear stress on the smooth sidewall (σ_1) should be less than the shear stress on the rough driving boundary (σ_0). The small rate dependence appears undetectable in our shear-force measurements, with the parameter α estimated to be well below 0.05.

[27] In the thesis work listed as Ref. [23], it is assumed that the sidewall resistance obeys a slip-speed dependence $\sigma^{\text{wall}} = g(v^{\text{slip}}) \approx \sigma_1[1+\beta \ln(v^{\text{slip}}/v_0^{\text{slip}})]$ and that v^{slip} can be approximated by the velocity of the horizontal sheets $V_x(z)$. Then an iteration gives $\ln[V_x(z)/V_x(0)] \sim (2\sigma_1/\alpha\sigma_0 W_0)\left[z + \frac{\beta}{2}(2\sigma_1/\alpha\sigma_0 W_0)z^2\right]$ at its second approximation. The convergence of the iteration scheme may require further work. Nevertheless, this approximation bears the same functional form as the quadratic relation that has been used to fit the master curve of velocity profiles in our measurements [Fig. 3(a)].

[28] P. A. Thompson and G. S. Grest, Phys. Rev. Lett. **67**, 1751 (1991). Note that their 2D simulations are performed in a context for which the gravity-induced gradient of normal stress is significant and the upper layers are sufficiently agitated: the imposed normal force is less than the weight of 24 layers of grains with the typical driving speed ranging from 22 to 53 $(gd)^{0.5}$; the packing thickness is about $10^2 d$. In our experiments, the imposed normal stress is more than the weight of 10^2 layers of grains while the highest driving speed is less than $10^{-2}(gd)^{0.5}$; the typical packing is 24 layers thick. The low speed and high normal load in our experiments renders the entire packing quasistatic. The shear banding and the "phase boundary" that occurs in our thick-layer experiments are induced mainly by sidewalls rather than by gravity.